ELSEVIER

#### Contents lists available at ScienceDirect

#### Water Research

journal homepage: www.elsevier.com/locate/watres



# RiSIM: River surface image monitoring software for quantifying floating macroplastic transport

Tomoya Kataoka <sup>a,b,\*</sup>, Takushi Yoshida <sup>c</sup>, Kenji Sasaki <sup>c</sup>, Yoshinori Kosuge <sup>d</sup>, Yoshihiro Suzuki <sup>d</sup>, Tim H.M. van Emmerik <sup>e</sup>

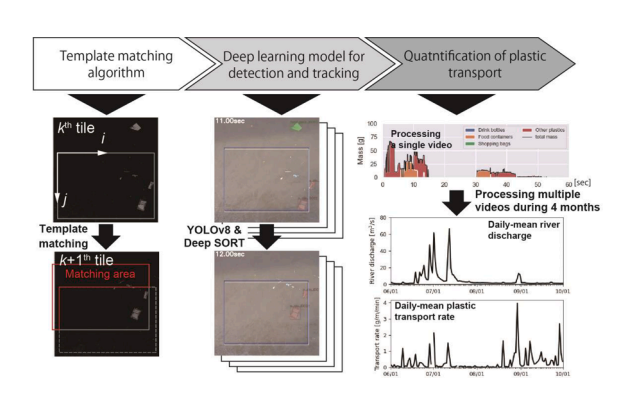
- <sup>a</sup> Department of Civil & Environmental Engineering, Ehime University, Matsuyama, Japan
- <sup>b</sup> Center for Marine Environmental Studies, Ehime University, Matsuyama, Japan
- <sup>c</sup> Business Planning and Development Division, Yachiyo Engineering Co., Ltd., Tokyo, Japan
- d Environmental Consulting Department, Environmental Management Unit, JAPAN NUS Co., Ltd., Tokyo, Japan
- <sup>e</sup> Wageningen University and Research, Hydrology and Environmental Hydraulics Group, Wageningen, The Netherlands

#### HIGHLIGHTS

- RiSIM, a river surface image monitoring software, was newly developed.
  RiSIM quantifies floating macroplastic
- transport on river surfaces.

   Deep learning models were imple-
- Deep learning models were implemented to detect and track floating plastics.
- Temporal variabilities in RiSIM-derived plastic transport matched ground truth data
- RiSIM revealed a significant relationship between plastic transport and discharge.

#### GRAPHICAL ABSTRACT



#### ARTICLE INFO

Keywords: Plastic pollution AI Remote sensing Marine litter Hydrology Japan

#### ABSTRACT

Reliable and continuous plastic monitoring in rivers is essential for quantifying plastic flux and guiding mitigation efforts. One effective strategy for observing floating plastic transport is image-based monitoring using deep learning models. We developed river surface image monitoring software (RiSIM) to quantify floating macroplastic transport through three core processes: (1) a template matching algorithm, which identifies matching areas in a frame that resemble a template given in the previous frame; (2) deep learning models for plastic detection, classification, and object tracking; and (3) the evaluation of plastic transport rate in terms of both quantity and mass. The RiSIM-derived plastic transport rates were validated through a mark-release-recapture experiment and *in-situ* visual observation under both non-flood and flood conditions. The temporal variability and composition of the plastic transport rate in terms of quantity and mass were in good agreement with the ground truth data (r = 0.91 and 0.80, respectively). And also, it remained valuable for capturing the temporal variability in plastic transport rate (r = 0.87) via the comparison with *in-situ* visual observation, indicating that the RiSIM is valuable for assessing the increase in plastic transport rate due to a flood event. In fact, we found a significant relationship ( $r^2 = 0.36$  for quantity;  $r^2 = 0.27$  for mass) between daily-mean plastic

<sup>\*</sup> Corresponding author at: Department of Civil & Environmental Engineering, Ehime University, 3 Bunkyo-cho, Matsuyama, Japan, 790-8577. *E-mail address:* kataoka.tomoya.ab@ehime-u.ac.jp (T. Kataoka).

transport rates and river discharge during flood events over four months. Accordingly, the RiSIM, as a near-field remote sensing technology, is a powerful tool for quantifying plastic transport and managing mis-managed plastic waste in river environments.

#### 1. Introduction

Macroplastic debris (>25 mm; (GESAMP, 2019)) transported from land via rivers is a dominant source of mismanaged plastic in marine environments (González-Fernández et al., 2023; Meijer et al., 2021; Strokal et al., 2023). Plastic transport in rivers is a key process to be considered when developing countermeasures for plastic pollution (Bergmann et al., 2023; van Emmerik et al., 2023). However, transport processes are complex due to horizontal and vertical mixing (Haberstroh et al., 2021; Vriend et al., 2023), fluid dynamics, and diverse polymer characteristics (Kooi et al., 2018), especially during floods (van Emmerik et al., 2023). For example, net sampling in the Rhine-Meuse delta showed that plastic concentrations (quantity/mass per unit water volume) were lower at mid-depth than near the water surface or bottom, and the surface concentration was substantially higher than that near the bottom (Blondel and Buschman, 2022). Plastic debris also shows cross-sectional variability along river width, influenced by flow velocity and/or winds (van Emmerik et al., 2018). Quantifying macroplastic transport at the water surface, the primary route of microplastic dissemination (Haberstroh et al., 2021), is thus crucial for evaluating riverine export (Jia et al., 2023).

Previous works quantified plastic transport mainly by visual observation or remote sensing (Hurley et al., 2023). Visual observation, in which floating plastics are counted as they pass through a river cross-section (van Emmerik et al., 2018), is the most common approach. Because it is time- and labor-intensive, recent studies have adopted computer vision techniques using fixed cameras (e.g., van Lieshout et al., 2020) or uncrewed aerial vehicles (UAVs) (e.g., Schreyers et al., 2024) to overcome these limitations. Increasingly, deep learning methods are applied to detect floating plastic debris (e.g., van Lieshout et al., 2020), enabling quantification of debris counts. Counts area valuable for assessing spatiotemporal variability (van Emmerik et al., 2022b) and comparing plastic transport (González-Fernández et al., 2023; Meijer et al., 2021). However, estimating mass from counts alone introduces large uncertainties (Hurley et al., 2023; Jia et al., 2023; Roebroek et al., 2022; van Emmerik et al., 2023). To reduce uncertainty, area-based quantification has been proposed (Kataoka and Nihei, 2020). We recently developed a You Only Look Once version 8 (YOLOv8) architecture with a semantic segmentation extension to evaluate the area covered by floating debris, combined with object detection to improve mass-based transport estimates (Kataoka et al., 2024).

Despite progress in detection, quantitative assessment of plastic transport remains limited. Transport rates require detecting and tracking debris across sequential video frames. In our earlier work, floating debris transport, including natural objects, was quantified using vertical-shoot videos with a color-based image analysis and a template matching algorithm (Kataoka and Nihei, 2020). First, pixels corresponding to floating debris were segmented from the background based on color differences, and the debris-covered area was evaluated in each frame. Next, template matching was applied to sequential frames to calculate the displacement of the debris. By combining the cumulative debris area with the total displacement, the transport area was estimated. However, a major limitation of this method was that plastics could not be distinguished from other types of floating objects.

Here, we propose river surface image monitoring software (RiSIM) to compute floating macroplastic transport in terms of both quantity and mass. RiSIM incorporates our YOLOv8-based detection model (Kataoka et al., 2024) within the earlier transport evaluation framework (Kataoka and Nihei, 2020) and introduces a tracking algorithm to link detections

across frames. We validate RiSIM using two approaches: a mark-release-recapture experiment (MRRE) and comparison with visual observations under non-flood and flood conditions. MRRE is used to validate both quantity- and mass-based transport rates, while comparison with visual observations assesses applicability as an alternative method. Finally, we examine the relationships between RiSIM-derived plastic transport rate and river discharge to evaluate its utility for long-term monitoring. RiSIM provides a unified framework for river surface monitoring, enabling simultaneous quantification of floating plastics at multiple sites, and can contribute to assessing riverine emissions and global plastic budgets. Noted that, to improve readability and ensure consistency, a list of all abbreviations used in this article is provided in Table 1.

#### 2. Methods

#### 2.1. Framework of RiSIM image processing

The RiSIM encompasses the following three core processes: (1) computation of the flow velocity via a template matching algorithm, (2) multiobject detection and tracking, and (3) quantification of the plastic transport rate (Fig. 1). The details of these core processes are described in the following sections.

#### 2.1.1. Template matching to compute flow velocities at the water surface

First, the flow velocity at the water surface is evaluated by applying a template matching algorithm to sequences of frames after the video data are divided into multiple frames with the original frame rate. In the present study, 900 frames are generated from the vertically shot video data given the original frame rate ( $f_0$ ) and shooting duration (t) of 30 fps and 60 s, respectively ( $N=t\times f_0$ ). Each frame is clipped to a tile image with a size of 1024 px  $\times$  1024 px. Notably, this preprocessing step is required for data input into the subsequent deep learning model. The pixel displacement between two consecutive tile images is estimated along the horizontal and vertical axes and then converted to a real metric distance via a ground sampling distance (GSD) defined by measuring a view distance until water surface. Finally, the flow velocity is computed via the original frame rate.

The flow velocities  $(v_x \text{ and } v_y)$  in the i and j directions can be computed from the pixel displacement, which occurs in the i and j di-

**Table 1**Table of abbreviations.

Acronym	Definition						
ADWP	Antecedent dry weather period						
$mAP_{50-95}$	Mean average precision calculated over IoU thresholds ranging from						
	0.50 to 0.95 at 0.05 intervals.						
COCO	Common objects in context						
Deep	Simple online and realtime tracking with a deep association metric						
SORT							
Fps	Frames per second						
GSD	Ground sampling distance						
GUI	Graphical user interface						
IoU	Intersection over union						
JSON	JavaScript object notation						
MRRE	Mark-release-recapture experiment						
PRIMOS	Plastic runoff identification, monitoring & observation software						
RGB	Red Green Blue						
RiSIM	River surface image monitoring software						
UAV	Uncrewed aerial vehicle						
WLGCAM	Camera system with ultrasonic water level gauge						
YOLOv8	You Only Look Once version 8						

T. Kataoka et al. Water Research 288 (2026) 124678

rections and is evaluated through a template matching processing (Text S1). The displaced pixels are used to determine the transport distance (dx, dy) on a metric scale via the GSD. The instantaneous flow velocity in the horizontal and vertical directions can be evaluated by dividing the transport distance between two sequential tile images into  $f_o$ . To mitigate uncertainties caused by template matching errors, spikes in instantaneous velocity exceeding three standard deviations are regarded as outliers and removed. These missing values are subsequently interpolated using the mean velocity in the recoding period. Notably, the uncertainty of mean flow velocity was validated at six sites in the catchment area of the Shigenobu River in the comparison to the measurement by the flow meter, which were 0.15 m/s of root mean square error and 29 % of scatter index (r = 0.92, p < 0.001; Text S2).

#### 2.1.2. Plastic object detection via an instance segmentation model

The YOLOv8 segment model retrained via the training dataset (8022 items from 7356 frames) (Kataoka et al., 2024) was implemented in the RiSIM as a deep learning model for detecting plastic objects in river surface images (Fig. 1). This model can classify four categories of plastic objects (drink bottles, food containers, shopping bags, and other plastics) in RGB tile images with sizes of 1024 px  $\times$  1024 px. Drink bottles, food containers and shopping bags are typical forms of disposal plastic waste that are found globally in aquatic environments. The category "other plastics" included a wide variety of items such as non-beverage bottle-shaped plastics (e.g., cleaner or cosmetics containers), bag-shaped plastics (e.g., food packaging or snack bags), and plastic fragments. On the basis of the available YOLOv8 architectures (YOLOv8n, YOLOv8s, YOLOv8m, YOLOv8l, and YOLOv8x), five segmentation models were developed (Kataoka et al., 2024). The YOLOv81 architecture displayed the best performance among the five architectures and was adopted as a detection model for plastic objects (Kataoka et al., 2024). Notably, the detection performance for plastic debris was 59 % mAP<sub>50-95</sub>, and the classification performance was 23 % mAP<sub>50-95</sub> across four categories (Kataoka et al., 2024), as shown in Table S1.

Following YOLOv8-based classification, postprocessing was performed to refine object categorization by removing duplicate classifications, discarding potential false positives (e.g., small objects), and unifying categories based on tracked objects. The YOLOv8 segmentation model occasionally classifies the same object into different categories. In cases in which different objects of the same type were classified in multiple categories, the most plausible category was determined on the basis of the intersection over union (IoU) of the corresponding bounding boxes. If the IoU between two bounding boxes was greater than 0.8, the category of the detected plastic object was determined, with a high confidence score. Furthermore, RiSIM allows users to configure a threshold for pixel area to reduce false positives. Specifically, objects with an area smaller than the threshold are disregarded. In this study, a threshold of 900 pixels was applied, based on the minimum size of the four categories observed in video data during flood events.

Moreover, even the same object can be classified into different categories across multiple frames. To ensure consistency in the categorization of detected objects, an object tracking algorithm, namely, simple online and real-time tracking with a deep association metric (Deep SORT) (Wojke and Bewley, 2018), was implemented (Fig. 1). Deep SORT is a powerful tracking tool that incorporates a deep learning model to track an object throughout sequential frames and can track false-negative objects via YOLOv8 by extracting appearance feature information. In the Deep SORT configuration, the maximum age of each object for tracking was 50, the maximum cosine threshold, which is a similarity limit used to compare the appearance features (128-dimensional vectors) of detected objects, was 0.3, and the maximum IoU distance, which is a measure used to compare how much two bounding boxes overlap, was 0.9 via trial and error. Note that the other parameters of Deep SORT were set to the default values. The YOLOv8-derived false-negative case does not include the information on its category name or segmentation mask area, even if it can be successfully tracked by Deep SORT. Thus, the category name in each false-negative case was updated with a mode value for each object, and the area was interpolated on the basis of the average of the segmentation mask areas detected by the YOLOv8 segment model. Moreover, the YOLOv8-derived false-positive case can be removed on the basis of the

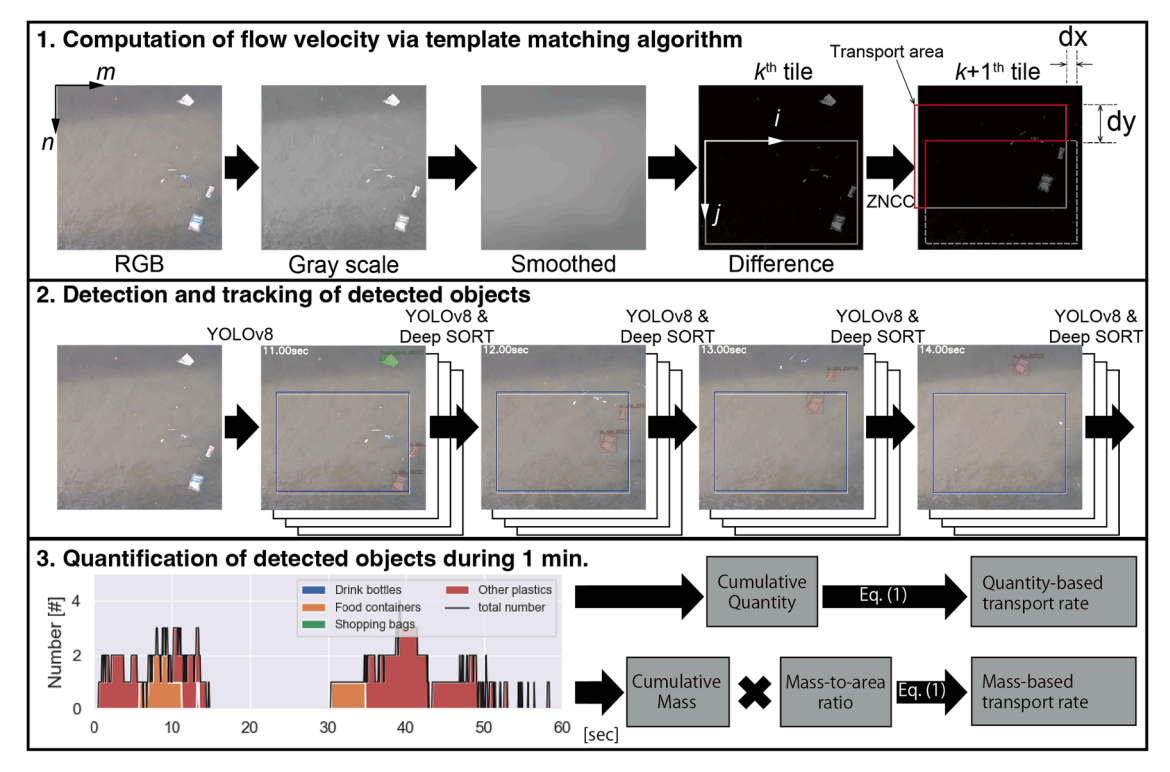


Fig. 1. Three steps of the RiSIM: Computation of the flow velocity, detection and tracking of plastic objects and quantification of the plastic transport rate.

tracking results of Deep SORT. In the present study, objects tracked fewer than three times were discarded as false positives.

Detection outputs from YOLOv8 segmentation model and Deep SORT, such as plastic debris classification, bounding boxes, confidence scores, segmentation masks, and pixel areas, are stored in the common objects in context (COCO) data format. This format, which uses Java-Script object notation (JSON) as a lightweight data-interchange standard, facilitates the storage of annotation information. Storing outputs in COCO format enables users to edit RiSIM outputs with existing annotation tools (e.g., <a href="https://supervisely.com/">https://supervisely.com/</a>), which can subsequently be used to fine-tune the YOLOv8 model. It should be noted, however, that in the present study we used only the original model without additional fine-tuning.

#### 2.1.3. Evaluation of the plastic flux via the RiSIM

The RiSIM can compute plastic transport rates in terms of quantity and mass on the basis of the following equations modified from the methodology of Kataoka and Nihei (2020).

$$F = \frac{\sum x_i}{\sum S_i} \times \frac{\sum A_i}{\Delta t \times (N-1)}$$
 (1)

where  $x_i$  denotes the quantity or mass of plastic objects found in each tile image and the subscript i is an index number of the tile image in the range between 0 and N. The mass of plastic objects is converted from the segmentation mask area identified by YOLOv8 segmentation model via the mass-to-area ratio (Fig. S1). N is the number of images based on the original frame rate of the video. For example, when the original frame rate was 15 fps (i.e., the time interval between two frames was 0.067 s),  $N = 60 \text{ s} \times 15 \text{ fps} = 900$ . The number of plastic objects was counted on the basis of object detection, for which YOLOv8l was applied. Moreover, the mass of the plastic object was evaluated via the segmentation mask generated via YOLOv8l, according to the method proposed by Kataoka and Nihei (2020). Considering the GSD, the segmentation mask was converted into a metric area, and then the mass was calculated by multiplying the mass-to-area ratio for each plastic category in YOLOv8l (Fig. S1).  $S_i$  was predefined based on the size of the tile image (1024 px × 1024 px). Hence, the first term represents the mean quantity/mass-based concentration of plastic objects calculated from all tile images.  $\Delta t$  is based on the optional frame rate (e.g., 0.2 s).  $A_i$  is the transport area in  $\Delta t$ , which is determined on the basis of the pixel displacement in images in the x-axis and y-axis directions via the template matching (Fig. 1).

#### 2.2. Mark-Release-Recapture experiment (MRRE)

The MRRE for floating macroplastic debris was conducted from 10:00–12:00 on July 18, 2024, at the Ishite River, Ehime Prefecture, Japan, to validate the quantity-based and mass-based plastic transport rates evaluated via the RiSIM (Fig. S2). The Ishite River is the largest tributary of the Shigenobu River, which is a class A river in Japan. In the

Ishite River Basin, a custom camera system with an ultrasonic water level gauge (WLGCAM) has been installed to monitor floating macroplastic debris on the river surface from a water pipe bridge over the river since July 20, 2023 (Text S3). On the survey date, the water depth was lower than 50 cm, which is the non-flood condition. During the MRRE, WLGCAM automatically recorded one-minute videos every 2 min. The plastic and nonplastic samples were collected and classified into five categories (drink bottles, food containers, shopping bags and other plastics), which are the same categories used in the YOLOv8 segmentation model (see 2.1.2). The quantities of items in these categories are listed in Table 2. One surveyor released the samples from upstream of the bridge, and two surveyors collected them downstream (Fig. S2).

The samples were released according to seven scenarios: three large, two medium and two small scenarios (Table 2). Considering the composition of the four categories in Japanese rivers (Kataoka et al., 2024), eighty, forty and twenty plastic samples were prepared in the large, medium and small scenarios, respectively. Unfortunately, several samples were not recorded in one-minute videos because the recording time ended; thus, the quantity and mass of the samples that were recorded are listed in Table 2. Note that the third large scenario (L3) was designed to confirm the robustness of the RiSIM under high-debris-supply conditions.

The quantity- and mass-based transport rates of the samples were evaluated by visually counting objects captured in the one-minute videos (Table 2). The quantity-based transport rate was computed by dividing the total number of captured samples by the recording time (one minute). Additionally, the mass-based transport rate was computed by dividing the total mass of the released samples measured by a weight scale in advance by the recording time. The total quantity and mass of the captured samples in each scenario are shown in Table 2.

Moreover, the quantity-based and mass-based plastic transport rates were estimated via RiSIM analyses with the same 1-min video on the basis of Eq. (1) (see 2.1.3). During the MRRE, the viewing distance from the WLGCAM was 7.04 m, and the GSD was 3.00 mm/px. Since the frame size was 4 K (3840 px  $\times$  2160 px), the total width and height of the frame were 11.52 m and 6.48 m, respectively (Fig. S3). Eighty percent of the total width (9.22 m) was determined as the target (red frame of Fig. S3). Note that we analyzed the frame by dividing it into three tiles because the width of the tile images input into YOLOv8 was 1024 px. The mass-based transport rate was derived from the cumulative area of the segmentation mask considering the corresponding GSD and mass-to-area ratio (Fig. S1).

#### 2.3. Visual observations during non-flood and flood conditions

The visual observation of floating macroplastic debris was conducted via the water pipe bridge installed in the WLGCAM system over the Ishite River to validate the plastic transport rate in actual situations in which an unknown amount of macroplastic debris is transported under non-flood and flood conditions (Fig. S4). To date, the quantification of macroplastic debris in river environments has been based on visual

**Table 2**The quantity and mass of plastic samples for the MRRE in 7 scenarios.

Scenarios	Prepared items	Number					Mass				
		Drink bottles	Food containers	Shopping bags	Other plastics	Total	Drink bottles	Food containers	Shopping bags	Other plastics	Total
Large 1 (L1)	80	9	0	8	26	43	275.6	0	21.8	385.4	682.8
Large 2 (L2)	80	5	8	4	20	37	123	51.5	13	517.9	705.4
Large 3 (L3)	80	5	5	5	22	37	157.6	41.5	14.7	563.8	777.6
Medium 1 (M1)	40	4	4	3	12	23	127	37.1	9.2	322	495.3
Medium 2 (M2)	40	3	2	2	12	19	84.7	13.4	5.4	319.6	423.1
Small 1 (S1)	20	3	3	1	7	14	105.1	27.6	1.7	146.9	281.3
Small 2 (S2)	20	2	1	2	6	11	73.7	14.2	5.4	170.6	263.9

T. Kataoka et al. Water Research 288 (2026) 124678

observation because of the advantages of this approach in terms of robustness and ease of implementation (Meijer et al., 2021; van Emmerik et al., 2023). Thus, we clarify whether the RiSIM can provide an alternative to visual observation for quantifying floating macroplastic debris through a comparison of both approaches.

Visual observation under non-flood conditions was carried out from 10:00-16:00 JST on June 26, 2024, with the aim of understanding the occurrence of false-positive cases. The maximum discharge in the observation date was 5.3 m<sup>3</sup>/s, which the return period (Text S4) did not exceed one year. The vertical distance from the bridge to the water surface was, on average, 6.9 m, with small fluctuations of approximately 0.04 m during the observation period. Three observers were arranged at three locations (sections A1 to C1) across the bridge simultaneously, and the plastic objects that passed through an approximately 7-m wide section (Fig. S4) for 1 min in a 10-min interval were visually counted. Owing to the vegetation coverage in the D1 section, which is 4 m wide, it was excluded from the observation scope. In total, 84 % of the river width (22 m of 26 m) was observed, while the plastic transport rate per unit width on the 'B1' section in the coverage of WLGCAM was used for validating RiSIM-based transport rate. The plastic objects were visually classified into four plastic categories, and visual counting was performed.

Moreover, visual observations under flood conditions, which is defined as a water level rise of >0.5 m within 10 min, were carried out from 8:30 to 15:30 JST on June 28, 2024, with the aim of understanding the change in the macroplastic transport rate during floods in comparison with that during non-flood conditions. The maximum river discharge in the observation date was 117.64 m<sup>3</sup>/s corresponding to 1.91 years of return period (Text S4). In terms of the increase in water level, the distance from the bridge was on average 5.6 m, with larger fluctuations of approximately 0.64 m than those under non-flood conditions. In the same manner as in the non-flood cases, the four observers at the four locations (B2 to D2 and F2) visually counted and classified the plastic objects that passed through approximately 7-m wide sections (Fig. S4) for 1 min in a 10-min interval. To avoid the influence of bridge columns, the A2 section, which is 7 m wide, and the E2 section, which is 4 m wide, were excluded from the observations. In total, 71 % of the river width (27 m of 38 m) was observed, while the plastic transport rate per unit width on the 'B2' section in the WLGCAM coverage was used for the validation.

The plastic transport was evaluated at 10-minute intervals by applying the RiSIM to the 1-min video data, followed by calculation of the hourly mean transport rates. The plastic transport rates were quantified by dividing each frame of the video into three 1024 px-square tile images with the RiSIM and then summing the rate from each tile image (see 2.2 and Fig. S3). Given that the monitoring width changed in response to water level fluctuations, normalization on the basis of the observed width was performed to estimate the plastic transport rate per unit width, enabling direct comparison with visual monitoring results. The observers were pretrained via the International Expert Meeting on Remote Sensing Technologies for Plastic Monitoring in Aquatic Environments (SmartMLRST) organized by the Ministry of the Environment, Japan (Isobe et al., 2025).

#### 2.4. Application of RiSIM to long-term monitoring for plastic transport

To demonstrate the ability of the model encompass hydrological conditions when estimating the plastic transport rate, we applied the RiSIM to 2752 1-min videos obtained by WLGCAM in the daytime (6:00–18:00) from June to September 2024 (Fig. S5). After the plastic transport rate from each video was computed, the hourly average transport rates were calculated to account for the varying recording intervals, which differed according to river conditions on the observation days (10 min during flood events and 60 min during non-flood periods; see Text S3). Since river discharge was not measured at the WLGCAM site, we simply calibrated the river discharge observed at

Yuwatari station on the basis of the time lag and catchment area ratio (Text S3). The time lag was measured based on the temporal fluctuations of water level at both sites. And the catchment areas at both sites were calculated by QGIS version 3.40.5 (https://qgis.org/).

#### 3. Results and discussion

#### 3.1. Estimation of image-based plastic transport in the MRRE

The image-based plastic transport rates output by the RiSIM were compared with the visual-based plastic transport rates (i.e., ground truth) from 10:00-12:00 JST on 18 July 2024 (Fig. 2). Note that the image-based and visual-based transport rates were normalized based on the width of the monitored area. The temporal variabilities in the quantity-based and mass-based transport rates quantified from the river surface videos were in good agreement with those calculated for the ground truth data (r=0.91 and 0.80; see Fig. 2a and b, respectively) according to Pearson's correlation analysis (Text S4). This demonstrated that the RiSIM was effective for quantifying the temporal variability of floating macroplastic debris from river surface videos. Nevertheless, the quantity-based transport rates were slightly overestimated relative to the ground truth, primarily due to the presence of false-positive detections and the reassignment of tracking identifiers to the same plastic debris across consecutive frames by Deep SORT (Fig. 2a).

The RiSIM categorization was compared with the ground truth (Fig. 2d). The primary and secondary plastic categories in terms of quantity were "other plastics" and "drink bottles", which were consistent with the ground truth data. The consistency in the item-wise numerical composition indicated the reliable performance of the RiSIM classification with YOLOv8 and Deep SORT. Moreover, "drink bottles" and "other plastics" accounted for the majority of the total mass (85 %), which was consistent with the ground truth (93 %) (Fig. 2d), but the item-wise mass composition between these two categories differed. In the RiSIM, "drink bottles" accounted for a larger proportion, whereas in the ground truth, "other plastics" was dominant. This discrepancy was likely due to using the mass-to-area ratio for mass estimation. In the present study, the average value of the mass-to-area ratio for mass conversion was used regardless of the mass-to-area ratio of the "other plastics" category, which exhibited substantial variability due to the diversity of plastic objects present (Fig. S1). In fact, the mean mass-toarea ratio of "other plastics" used for mass conversion in the present study (0.038 g/cm<sup>2</sup>) was one order of magnitude lower than that observed in the MRRE (0.20 g/cm<sup>2</sup>). Consequently, the mass ratio of the "other plastics" category estimated with the RiSIM may have been underestimated. As one of the solutions, the categorization by YOLOv8 can potentially be subdivided. In contrast, as our previous works demonstrated, the subdivision of categories could yield an increase in false-positive and false-negative cases (Kataoka et al., 2024). Hence, enhancing the categorization performance of YOLOv8 via the fine-tuning of the current model should be explored in the future.

Furthermore, we found a discrepancy in the mass estimation results when the mass-to-item ratio was used (Fig. S1). Instead of the use of the mass-to-area ratio, we converted the quantity-based plastic transport rate to mass-based plastic transport via the mass-to-item ratio. As expected, the temporal variability in the mass-based plastic transport rate was consistent with that based on the ground truth data ( $r=0.73,\,p<0.001;\,Fig.\,2c$ ), whereas the composition of the plastic types differed from the ground truth composition (Fig. 2d). Notably, drink bottles were dominant in terms of mass (70 %), which can be attributed to their greater mass-to-item ratio than other items (Fig. S1). Compared with the ground truth observations (26 %), the plastic transport of drink bottles appeared to be overestimated. This result suggests that mass conversion based on mass-to-item ratios is associated with higher uncertainty when estimating plastic transport, whereas mass-to-area-based conversion provides a more reliable approach for quantifying plastic transport.

Nevertheless, we successfully constrain the temporal variabilities of

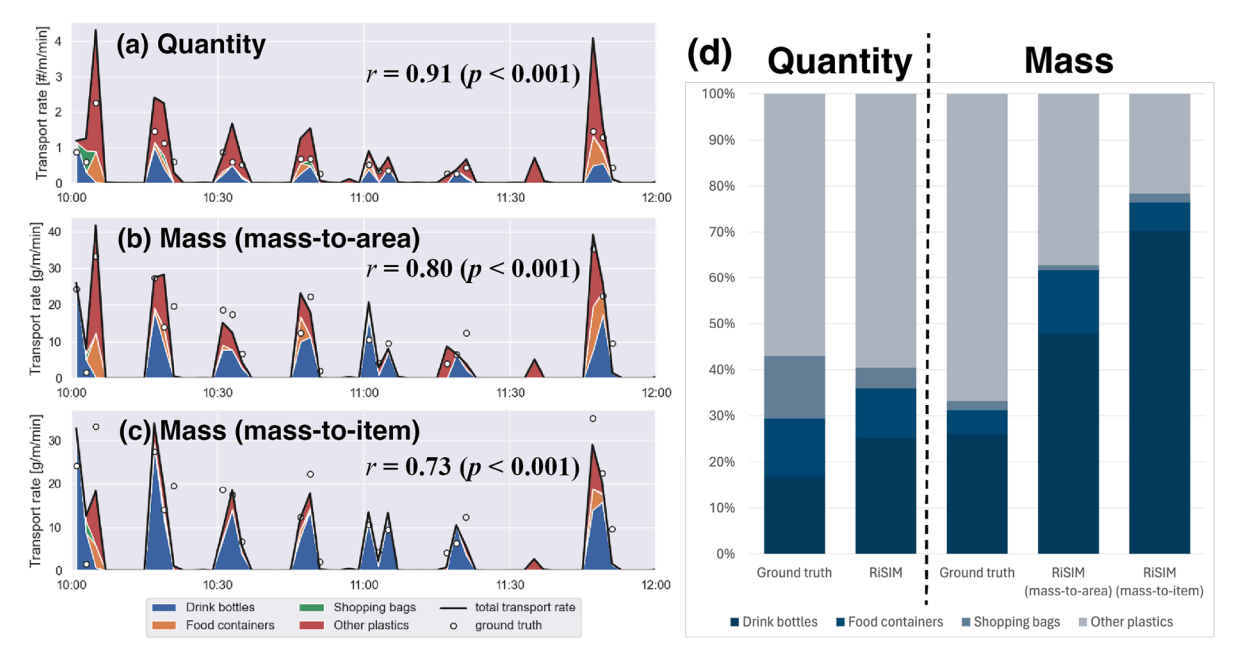


Fig. 2. Temporal variability in plastic transport (a)-(c) and item composition of plastic debris (d). The quantity-based plastic transport rate is shown in panel (a), and the mass-based transport rates converted on the basis of mass-to-area and mass-to-item ratios are shown in panels (b) and (c), respectively. The stacked time series in panels (a)-(c) shows the RiSIM-based plastic transport rate for each category, and the white circles denote the ground truth. The compositions of the ground truth and RiSIM-identified plastic objects are shown in panel (d).

both number-based and mass-based transport rates through the RiSIM (Fig. 2a and b). The harmonization of monitoring methods is crucial, particularly during flood events, for understanding the outflow and transport processes of plastic objects from terrestrial areas. However, in situ visual observation is accompanied by challenges in terms of the continuity and safety of the surveys.

### 3.2. Applicability of the RiSIM to videos obtained under non-flood and flood conditions

Under non-flood conditions (June 26, 2024), very little plastic debris was quantified through visual observation, with an average transport rate of 0.03 $\pm$ 0.02 #/m/min (Fig. 3). Similarly, the RiSIM yielded very low transport rates, with an average transport rate of 0.03 $\pm$ 0.02 #/m/

min. In contrast, a significantly greater amount of plastic debris was detected during flood events (June 28, 2024) than during non-flood events, which was consistent with the transport rates derived from both in situ visual observations and the RiSIM (Fig. 3). On the basis of in situ visual observations, the number-based transport rate averaged at the daily scale (0.27 $\pm$ 0.25 #/m/min) was approximately ten times greater than that during the non-flood conditions (0.03 $\pm$ 0.02 #/m/min). Consistently, the average transport rate estimated via the RiSIM (0.36 $\pm$ 0.28 #/m/min) was approximately ten times higher than that during non-flood conditions (0.03 $\pm$ 0.02 #/m/min) and significantly greater than that obtained via visual observation.

In fact, the RiSIM-derived plastic transport rates were significantly correlated with visually observed plastic transport rates ( $r=0.87,\,p<0.001;\,$  Fig. 3) via Pearson's correlation analysis (Text S4), which

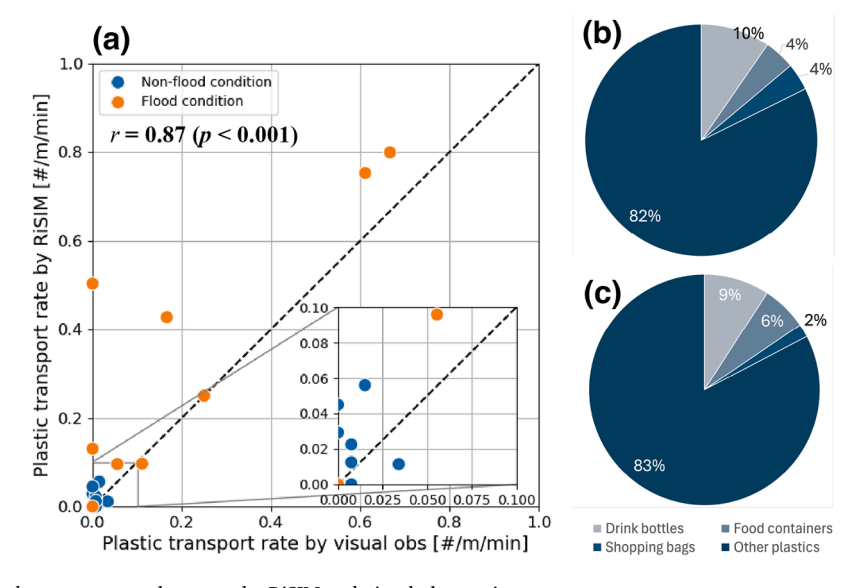


Fig. 3. Comparison of numerical transport rates between the RiSIM and visual observation.

The compositions of the plastic categories identified with the RiSIM and visual observation are shown in panels (b) and (c), respectively.

T. Kataoka et al. Water Research 288 (2026) 124678

demonstrated that the RiSIM is a valuable tool for evaluating the temporal variability of plastic transport via remote sensing. While the RiSIM-derived plastic transport rates were overestimated compared with the visually observed rates (Fig. 3), this outcome can be attributed to several potential causes. As the water level ranged from 7.0 to 7.9 m during flood condition, the monitoring section of RiSIM was changed depending on water level. The difference in monitoring section could affect to the evaluation of plastic transport rate. Moreover, in situ visual observations from the bridge might not account for all debris, as the high flow velocities range from 0.81 to 2.72 m/s. Some objects were ambiguous with respect to plastic identification (Fig. S6); however, their classification as plastic debris likely depends on subjective interpretation. Unlike visual observation, which may be prone to observer bias, AI-based systems such as the RiSIM ensure consistency and objectivity in plastic detection.

#### 3.3. Relationship between the plastic transport rate and hydrology

The hourly quantity-based and mass-based plastic transport rates fluctuated considerably with increasing river discharge (Fig. 4a and 4b, respectively). The maximum river discharge over the four months was  $145.42 \, \mathrm{m}^3/\mathrm{s}$  corresponding to 2.35 years of return period estimated using the Log-Pearson Type III distribution (Text S4). The hourly plastic transport rates greatly fluctuated at river discharge rates lower than 9.47  $\,\mathrm{m}^3/\mathrm{s}$  corresponding to about 1 year of return period (i.e., T=1.01 in Eq. S9; see Text S4) (see gray dots in Fig. 4a and b), highlighting poor regression performance under low-discharge conditions, as reported in several previous works (Aulenbach et al., 2016; Moatar et al., 2017). Although several alternative approaches for establishing reliable regression equations for environmental loads (e.g., sediment and

nutrients) have been suggested, we do not discuss these approaches because the aim of the present study is to develop an image-based monitoring approach. Thus, when focusing on river discharge rates greater than 9.47  $\rm m^3/s$ , we can perform a regression of the plastic transport rate on the basis of discharge by the following equation,

$$L = 10^a Q^b \tag{2}$$

where L is the quantity-based or mass-based plastic transport rate and Q is the calibrated river discharge. The regression coefficients a and b are shown in Table 3. The hourly quantity-based and mass-based plastic transport rates were effectively regressed ( $r^2 = 0.29$  and  $r^2 = 0.20$ , respectively; Table 3). The coefficient b represents the slope of the loglog plain, which was slightly greater for the quantity-based plastic transport rate than for the mass-based rate (Table 3), but a Z test (Text S4) indicated no statistically significant difference (z = 1.40, p > 0.05).

The daily-mean plastic transport rate can be also associated with the daily-mean river discharge (Fig. 4c and d). The daily-mean plastic transport rate fluctuated when the daily-mean river discharge was

 Table 3

 Regression coefficients determined via a linear regression method.

	n	$R^2$	$a\pm$ 95 % C.I.	$b\pm95$ % C.I.				
Hourly plastic transport rate								
Quantity based	101	0.29	$-3.35 {\pm} 0.64$	$1.40 {\pm} 0.43$				
Mass based	101	0.20	$-2.65 \pm 0.76$	$1.29{\pm}0.52$				
Daily plastic transport rate								
Quantity based	24	0.36	$-2.81 {\pm} 0.68$	$0.95{\pm}0.56$				
Mass based	24	0.27	$-2.24 {\pm} 0.78$	$0.89{\pm}0.64$				

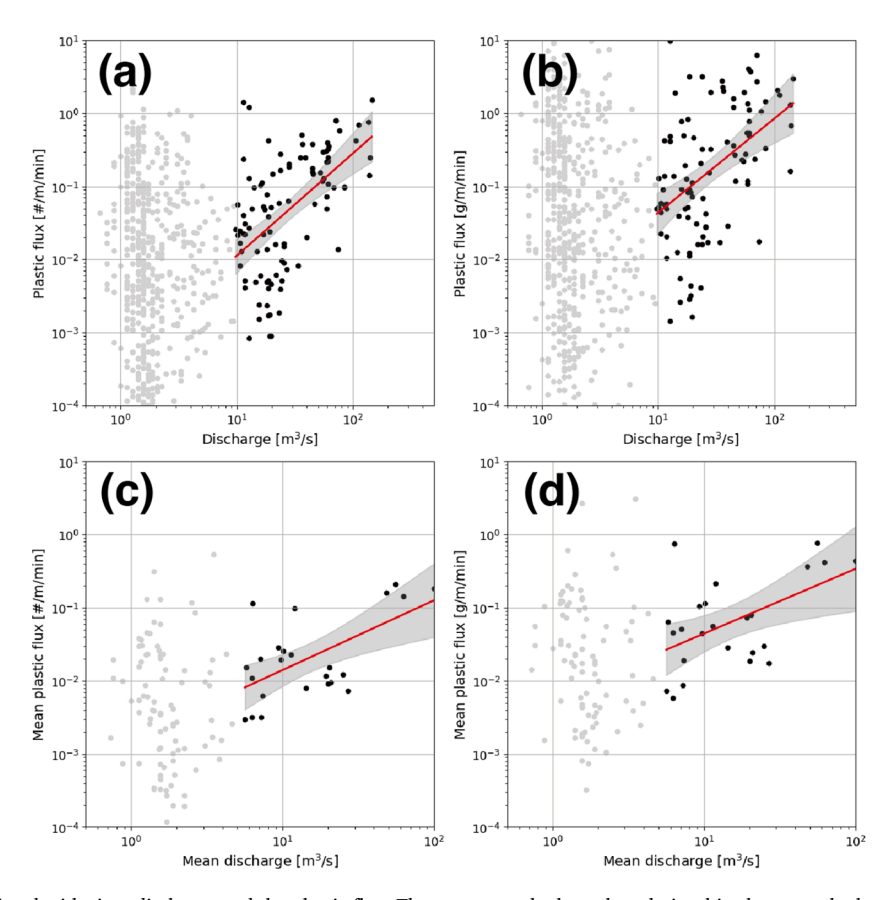


Fig. 4. L-Q equations associated with river discharge and the plastic flux. The upper panels show the relationships between the hourly river discharge and plastic transport rates in terms of quantity (a) and mass (b). The lower panels denote the relationship between the daily mean river discharge and plastic transport rates for quantity (c) and mass (d). The gray plots indicate the plastic transport rates when the river discharge is lower than 9.47  $\text{m}^3$ /s for panels (a) and (b) and 5.61  $\text{m}^3$ /s for panels (c) and (d). The red line and gray area indicate the L-Q equation and 95 % confidence interval of the equation, respectively.

smaller than 5.61 m³/s corresponding to about 1 year of return period (i. e., T=1.01 in Eq. S9; see Text S4). Interestingly, when the daily-mean plastic transport rate and river discharge were computed, the relationship significantly improved ( $r^2=0.36$  for number and  $r^2=0.27$  for mass; Table 3). The coefficient b for both the quantity-based and mass-based plastic transport rates was approximately 0.9 (Table 3), and there was no statistically significant difference via the Z test (z=1.14, p>0.05). These results indicate that the quantity-based and mass-based transport rates similarly vary with river discharge.

Nevertheless, overall correlations between plastic transport and river discharge remained low, reflecting the high variability in transport responses to discharge fluctuations. Similar to organic pollutant transport (e.g., Peter et al., 2020), longer antecedent dry weather periods (ADWP) promote greater accumulation of plastic debris in the watershed, resulting in higher transport during subsequent flood events, that is a first flush effect. Conversely, when the ADWP is short, the transported plastic load is expected to be lower. For example, the RiSIM-derived plastic transport in late August exceeded that in July despite non-extreme floods, owing to the longer ADWP observed (Fig. S5). Moreover, plastic transport during the rising stage of flood events often exceeds that during the falling stage, even at similar discharge levels (Peter et al., 2020). Hence, low correlations are common under non-extreme conditions, because plastic transport is primarily limited by supply rather than discharge (Roebroek et al., 2022; van Emmerik et al., 2022a). Hydrological thresholds such as bank overtopping or sewer overflow must be exceeded to increase the available plastic supply, but in the absence of such thresholds, low correlations can be expected.

### 3.4. Future outlook of remote sensing for quantifying floating plastic transport at the surface of Rivers

In this study, we established a method for quantifying the transport of plastic debris floating on river surfaces via vertically captured video data. The RiSIM is innovative in two key aspects: deep learning-based detection and tracking functions are provided for plastic debris on the water surface, and the surface flow velocity is measured with a template matching algorithm. This allows for efficient monitoring of the transport rate of floating plastic.

To date, numerous researchers have conducted visual counting studies from bridges (González-Fernández et al., 2021; Lou et al., 2023; Moss et al., 2021; Pinto et al., 2023; Schreyers et al., 2021; van Emmerik et al., 2023; van Lieshout et al., 2020). Visual counting is easy to perform and can be performed anywhere, as it involves only recording the characteristics (e.g., types and colors) of floating objects directly on site. This approach is also robust, applicable to a variety of rivers, and can yield reasonably reliable data if well-trained observers are involved (van Emmerik et al., 2023). Nevertheless, the observation data are inherently subject to observer bias, thereby limiting objectivity. Moreover, onsite visual counting involves considerable safety risks during flood events, when a large outflow of plastic debris may occur (van Emmerik et al., 2023). Additionally, since observers must remain on site during monitoring, the method is time and labor intensive, resulting in limited sustainability for long-term and/or multisite monitoring (van Lieshout et al., 2020).

The RiSIM is expected to serve as a powerful tool for clarifying the emission of macroplastic debris transported via river systems and serves to overcome the limitations of onsite visual counting. Specifically, observer bias can be minimized by implementing a deep learning model for detecting and counting floating macroplastics, thereby enhancing objectivity. In addition, the installation of a fixed camera at a bridge enables safe observation even during high-flow conditions. In fact, we successfully observed the temporal variability in the plastic transport rate regardless of flood conditions (Fig. S5) and consequently demonstrated that the proposed method is effectively encompasses hydrological conditions (red line in Fig. 4). The hydrological factors related to plastic transport are also valuable for managing plastic waste in river

basins and for evaluating the effectiveness of mitigation strategies. For example, in this study, the slope of the regression equation for daily mass-based plastic transport was approximately 1.2 (Table 3). If post-intervention monitoring, such as litter cleanup efforts within the watershed, revealed a reduced slope, it would indicate the effectiveness of such measures in suppressing plastic outflows from land areas. Therefore, the RiSIM can support continuous, long-term monitoring across multiple sites and is considered a promising tool for managing the outflow of macroplastics from terrestrial sources and implementing countermeasures for reducing plastic loads.

Furthermore, during flood events, rising water levels can reduce the GSD of video footage. To address this technical challenge, we implemented the WLGCAM. Owing to the decrease in GSD during high-flow conditions, the monitoring width becomes narrower, preventing consistent evaluation of plastic transport from the non-flood to flood stages. To address this limitation, in the present study, the GSD was calculated on the basis of water level measurements obtained from an ultrasonic water level sensor, and the plastic transport rate per unit width was successfully quantified. Accordingly, a significant relationship with river discharge (Fig. 4) was established, and the monitoring width ranged between 7.1 m (GSD: 2.33 mm/px) and 9.7 m (GSD: 3.33 mm/px). Moreover, by accounting for GSD fluctuations caused by water level changes, the area-based plastic transport rate was estimated. Specifically, by multiplying the area-based transport rate by the mass-toarea ratio, mass-based transport was estimated. Mass conversion can provide more reliable estimates of mass-based transport rates than can mass conversion on the basis of the mass-to-item ratio (see 3.1).

We have developed and released PRIMOS (Plastic Runoff Identification, Monitoring & Observation Software), a cloud-based monitoring system for floating riverine debris that incorporates the RiSIM framework (https://info.river-monitoring.net/en/index.html). Since PRIMOS operates through a standard web browser, no local environment setup is required. The integration of RiSIM into a cloud-based graphical user interface (GUI) platform enables users to conduct plastic transport analyses with minimal technical effort. Moreover, because all computations are performed on the server side, no high-performance computing resources are needed on the user's device, making the system both accessible and efficient. We anticipate that PRIMOS will serve as a conventional tool for plastic transport monitoring in riverine environments.

Nonetheless, two technical challenges remain in quantifying plastic transport using the RiSIM. First, the applicability of the RiSIM must be validated across multiple rivers worldwide and under extreme conditions. In this study, the YOLOv8 model for plastic detection developed by Kataoka et al. (2024) was applied, but the current performance of plastic classification remains limited (Kataoka et al., 2024), introducing uncertainty into mass-based transport estimates. Indeed, the mass composition of plastic items, as validated by the MRRE, displayed discrepancies from the ground truth (Fig. 2d). To improve classification performance, strategies such as fine-tuning the YOLOv8 model or further subdividing classification categories should be considered when applying the RiSIM to diverse river environments in the future. In addition, floating plastics may be partially submerged, degraded, or trapped within clusters of natural materials. Although some of these items can still be detected and evaluated depending on their shape (Fig. S6), fully capturing all partially visible plastics remains challenging. Such efforts may increase the likelihood of false positives, even with a trained YOLOv8 model. Nonetheless, recent studies have actively explored deep learning approaches for detecting and classifying floating plastic debris (Astorayme et al., 2024; Jia et al., 2023). As these technologies are rapidly advancing, more accurate and robust models are expected to become available in the near future. Since the deep learning model embedded in RiSIM can be readily updated or replaced, RiSIM has strong potential as a flexible platform for integrating state-of-the-art models, thereby enhancing the reliability and accuracy of plastic transport estimation.

Another challenge lies in the limited observational coverage during floods due to the use of vertically oriented cameras deployed from bridges. In such cases, the monitoring width is narrow, leading to reduced representativeness of plastic transport estimates. While a relatively narrow river channel was considered in this study (20–91.5 m; see Text S3), this limitation would become even more pronounced for large rivers. Ideally, the cross-sectional profile of plastic transport should be monitored by installing multiple cameras laterally across the channel or utilizing aerial video captured by UAVs. In future studies, we will attempt to adopt the integrated monitoring framework proposed by van Emmerik et al. (2018) to estimate total plastic transport across cross-sections via the RiSIM.

#### 4. Conclusion

We developed the RiSIM to quantify floating macroplastic transport through three core processes: (1) a template matching algorithm; (2) deep learning models for plastic detection, classification, and object tracking; and (3) the quantification of plastic transport in terms of both quantity and mass via vertically recorded video data. The template matching algorithm was employed to compute the surface flow velocity via analyses of consecutive frames with a known ground sampling distance (GSD). Four typical types of plastic debris (drink bottles, food containers, shopping bags, and other plastics) were detected/categorized with the pretrained YOLOv8 mode with a segmentation extension and then tracked via simple online and real-time tracking with Deep SORT. The YOLOv8 segmentation model was used to evaluate the massbased plastic transport rate via the mass-to-area ratios of the four plastic categories as well as the quantity-based plastic transport rate. The detected plastic objects were consistently tracked by Deep SORT. Finally, the quantity-based and mass-based plastic transport rates were computed by processing all consecutive frames of video data.

The RiSIM-derived plastic transport rates were validated through an MRRE in which the four categories of plastic debris were intentionally released from upstream in a river and subsequently recaptured downstream. The temporal variation and item composition of the quantity-based and mass-based plastic transport rates were in good agreement with the true values (r = 0.91 and 0.80, respectively), although they were slightly overestimated. In addition, the RiSIM effectively modeled both the temporal variability and item-wise composition of plastic transport in terms of mass.

To demonstrate the applicability of the RiSIM under different hydrological conditions, we compared the plastic transport rate with in situ visual observations under both non-flood and flood conditions and then attempted to establish the relationship between the plastic transport rate and river discharge. The temporal variability of the RiSIM-derived plastic transport rate was consistent with that quantified on the basis of visual observation (r = 0.87), indicating that the RiSIM is valuable for assessing changes in plastic transport due to a flood event. The RiSIM-based plastic transport rates, in terms of quantity and mass, were significantly associated with high river discharge when the RiSIM was applied to the recorded video data for the four months from June to September 2024.

Accordingly, the RiSIM supports the more efficient and safe monitoring of the floating plastic transport rate than does the conventional in situ visual observation method. RiSIM-based continuous monitoring at multiple sites is a promising approach for managing the outflow of macroplastics from terrestrial sources and implementing countermeasures for reducing plastic loads. In the future, we will explore the applicability of the RiSIM to quantify-based plastic transport in various rivers worldwide. Accordingly, we expect that the RiSIM can greatly contribute to harmonizing the monitoring of floating plastic debris in rivers, as an important tool for quantifying plastic emission and transport in river environments and plastic budgets at the global scale.

#### **Funding**

This work was supported by the Environment Research and Technology Development Fund (JPMEERF21S11900 and JPMEERF20231004) of the Environmental Restoration and Conservation Agency of Japan, KAKENHI (24K00992), and a project (JPNP18016) commissioned by the New Energy and Industrial Technology Development Organization (NEDO).

#### Data availability

All data supporting the findings of this study are available in the supplementary information (Excel files). Video data are available from the corresponding author upon reasonable request. The RiSIM code will be made available from the corresponding author on reasonable request.

### Declaration of generative AI and AI-assisted technologies in the writing process

During the preparation of this work the authors used ChatGPT provided by Open AI in order to improving language and readability. After using this service, the authors reviewed and edited the content as needed and takes full responsibility for the content of the publication.

#### CRediT authorship contribution statement

Tomoya Kataoka: Writing – original draft, Visualization, Validation, Supervision, Software, Project administration, Methodology, Investigation, Funding acquisition, Formal analysis, Data curation, Conceptualization. Takushi Yoshida: Software, Investigation, Formal analysis, Data curation. Kenji Sasaki: Writing – review & editing, Software, Investigation, Formal analysis, Data curation. Yoshinori Kosuge: Writing – review & editing, Investigation, Formal analysis, Data curation. Yoshihiro Suzuki: Writing – review & editing, Investigation, Formal analysis, Data curation. Tim H.M. van Emmerik: Writing – review & editing, Methodology, Investigation, Data curation.

#### **Declaration of competing interest**

The authors declare that the research was conducted in the absence of any commercial or financial relationships that could be construed as potential conflicts of interest.

#### Acknowledgments

The authors are grateful to all the technical staff at Yachiyo Engineering Co., Ltd., and the students in the Informatics for Civil Engineering Laboratory of Ehime University to generate a training dataset. Furthermore, a part of this study utilizes the results of demonstration tests conducted under a project commissioned by the Ministry of the Environment of Japan in fiscal year 2024. We would like to express our appreciation to all the technical staff at Clealink Technology Co., Ltd., for their cooperation in the installation and operation of the WLGCAM.

#### Supplementary materials

Supplementary material associated with this article can be found, in the online version, at doi:10.1016/j.watres.2025.124678.

#### Data availability

Data will be made available on request.

## T. Kataoka et al. References

- Astorayme, M.A., Vázquez-Rowe, I., Kahhat, R., 2024. The use of artificial intelligence algorithms to detect macroplastics in aquatic environments: a critical review. Sci. Total Env. 945, 173843.
- Aulenbach, B.T., Burns, D.A., Shanley, J.B., Yanai, R.D., Bae, K., Wild, A.D., Yang, Y., Yi, D., 2016. Approaches to stream solute load estimation for solutes with varying dynamics from five diverse small watersheds. Ecosphere 7 (6), e01298.
- Bergmann, M., Arp, H.P.H., Carney Almroth, B., Cowger, W., Eriksen, M., Dey, T., Gündoğdu, S., Helm, R.R., Krieger, A., Syberg, K., Tekman, M.B., Thompson, R.C., Villarrubia-Gómez, P., Warrier, A.K., Farrelly, T., 2023. Moving from symptom management to upstream plastics prevention: the fallacy of plastic cleanup technology. One Earth. 6 (11), 1439–1442.
- Blondel, E., Buschman, F.A., 2022. Vertical and horizontal plastic litter distribution in a bend of a tidal river. Front. Environ. Sci. 10.
- GESAMP, 2019. Guidelines for the monitoring and assessment of plastic litter and microplastics in the ocean. GESAMP Rep. Stud. 99, 130.
- González-Fernández, D., Cózar, A., Hanke, G., Viejo, J., Morales-Caselles, C., Bakiu, R., Barceló, D., Bessa, F., Bruge, A., Cabrera, M., Castro-Jiménez, J., Constant, M., Crosti, R., Galletti, Y., Kideys, A.E., Machitadze, N., Pereira de Brito, J., Pogojeva, M., Ratola, N., Rigueira, J., Rojo-Nieto, E., Savenko, O., Schöneich-Argent, R.I., Siedlewicz, G., Suaria, G., Tourgeli, M., 2021. Floating macrolitter leaked from Europe into the ocean. Nat. Sustain. 4 (6), 474–483.
- González-Fernández, D., Roebroek, C.T.J., Laufkötter, C., Cózar, A., van Emmerik, T.H. M., 2023. Diverging estimates of river plastic input to the ocean. Nat. Rev. Earth. Environ. 4 (7), 424–426.
- Haberstroh, C.J., Arias, M.E., Yin, Z., Sok, T., Wang, M.C., 2021. Plastic transport in a complex confluence of the Mekong River in Cambodia. Env. Res. Lett. 16 (9), 095009.
- Hurley, R., Braaten, H.F.V., Nizzetto, L., Steindal, E.H., Lin, Y., Clayer, F., van Emmerik, T., Buenaventura, N.T., Eidsvoll, D.P., Økelsrud, A., Norling, M., Adam, H. N., Olsen, M., 2023. Measuring riverine macroplastic: methods, harmonisation, and quality control. Water. Res., 119902
- Isobe, A., Aliani, S., Andriolo, U., Dierssen, H., Game Monteiro, J., Goncalves, G., Hidaka, M., Kako, S.i., Kataoka, T., Martinez-Vincente, V., Matsuoka, D., Mishra, P., Streett, D., Takahashi, Y., Topouzelis, K., Van Emmerik, T., 2025. The Guidelines for Harmonizing Marine Litter Monitoring Methods Using Remote Sensing Technologies, Version 2.0. Ministry of the Environment Japan, Tokyo, Japan, p. 209.
- Jia, T., Kapelan, Z., de Vries, R., Vriend, P., Peereboom, E.C., Okkerman, I., Taormina, R., 2023. Deep learning for detecting macroplastic litter in water bodies: a review. Water. Res. 231, 119632.
- Kataoka, T., Nihei, Y., 2020. Quantification of floating riverine macro-debris transport using an image processing approach. Sci. Rep. 10 (1), 2198.
- Kataoka, T., Yoshida, T., Yamamoto, N., 2024. Instance segmentation models for detecting floating macroplastic debris from river surface images. Front. Earth. Sci.
- Kooi, M., Besseling, E., Kroeze, C., van Wezel, A.P., Koelmans, A.A., 2018. In: Wagner, M., Lambert, S. (Eds.), Freshwater Microplastics: Emerging Environmental Contaminants?. Springer International Publishing, Cham, pp. 125–152.
- Lou, F., Wang, J., Sima, J., Lei, J., Huang, Q., 2023. Mass concentration and distribution characteristics of microplastics in landfill mineralized refuse using efficient quantitative detection based on Py-GC/MS. J. Hazard. Mater. 459, 132098.

- Meijer, L.J.J., van Emmerik, T., van der Ent, R., Schmidt, C., Lebreton, L., 2021. More than 1000 rivers account for 80% of global riverine plastic emissions into the ocean. Science Advances 7 (18), eaaz5803.
- Moatar, F., Abbott, B.W., Minaudo, C., Curie, F., Pinay, G., 2017. Elemental properties, hydrology, and biology interact to shape concentration-discharge curves for carbon, nutrients, sediment, and major ions. Water Resources Research 53 (2), 1270–1287.
- Moss, K., Allen, D., González-Fernández, D., Allen, S., 2021. Filling in the knowledge gap: observing MacroPlastic litter in South Africa's rivers. Mar. Pollut. Bull. 162, 111876.
- Peter, K.T., Hou, F., Tian, Z., Wu, C., Goehring, M., Liu, F., Kolodziej, E.P., 2020. More than a first flush: urban creek storm hydrographs demonstrate broad contaminant pollutographs. Env. Sci. Technol. 54 (10), 6152–6165.
- Pinto, R.B., Barendse, T., van Emmerik, T., van der Ploeg, M., Annor, F.O., Duah, K., Udo, J., Uijlenhoet, R., 2023. Exploring plastic transport dynamics in the Odaw river, Ghana. Front. Environ. Sci. 11.
- Roebroek, C.T.J., Laufkötter, C., González-Fernández, D., van Emmerik, T., 2022. The quest for the missing plastics: large uncertainties in river plastic export into the sea. Env. Pollut. 312, 119948.
- Schreyers, L., van Emmerik, T., Nguyen, T.L., Phung, N.-A., Kieu-Le, T.-C., Castrop, E., Bui, T.-K.L., Strady, E., Kosten, S., Biermann, L., van den Berg, S.J.P., van der Ploeg, M., 2021. A field guide for monitoring riverine macroplastic entrapment in water hyacinths. Front. Environ. Sci. 9.
- Schreyers, L.J., van Emmerik, T.H.M., Bui, T.-K.L., Biermann, L., Uijlenhoet, R., Nguyen, H.Q., Wallerstein, N., van der Ploeg, M., 2024. Water hyacinths retain river plastics. Env. Pollut. 356, 124118.
- Strokal, M., Vriend, P., Bak, M.P., Kroeze, C., van Wijnen, J., van Emmerik, T., 2023. River export of macro- and microplastics to seas by sources worldwide. Nat. Commun. 14 (1), 4842.
- van Emmerik, T., de Lange, S., Frings, R., Schreyers, L., Aalderink, H., Leusink, J., Begemann, F., Hamers, E., Hauk, R., Janssens, N., Jansson, P., Joosse, N., Kelder, D., van der Kuijl, T., Lotcheris, R., Löhr, A., Mellink, Y., Pinto, R., Tasseron, P., Vos, V., Vriend, P., 2022a. Hydrology as a driver of floating river plastic transport. Earths. Future 10 (8), e2022EF002811.
- van Emmerik, T., Kieu-Le, T.-C., Loozen, M., van Oeveren, K., Strady, E., Bui, X.-T., Egger, M., Gasperi, J., Lebreton, L., Nguyen, P.-D., Schwarz, A., Slat, B., Tassin, B., 2018. A methodology to characterize riverine macroplastic emission into the ocean. Front. Mar. Sci. 5 (372).
- van Emmerik, T., Mellink, Y., Hauk, R., Waldschläger, K., Schreyers, L., 2022b. Rivers as plastic reservoirs. Front. Water. 3.
- van Emmerik, T.H.M., Frings, R.M., Schreyers, L.J., Hauk, R., de Lange, S.I., Mellink, Y.A. M., 2023. River plastic transport and deposition amplified by extreme flood. Nat. Water 1 (6), 514–522.
- van Lieshout, C., van Oeveren, K., van Emmerik, T., Postma, E., 2020. Automated river plastic monitoring using deep learning and cameras. Earth. Space Sci. 7 (8), e2019EA000960.
- Vriend, P., Schoor, M., Rus, M., Oswald, S.B., Collas, F.P.L., 2023. Macroplastic concentrations in the water column of the river Rhine increase with higher discharge. Sci. Total Env. 900, 165716.
- Wojke, N. and Bewley, A. 2018 Deep cosine metric learning for person re-identification, pp. 748–756.